Original Article | Journal of Biosystems Engineering

J. Biosyst. Eng. 43(2):94-102. (2018. 6)
https://doi.org/10.5307/JBE.2018.43.2.094

eISSN : 2234-1862
pISSN : 1738-1266

Development of Super-capacitor Battery Charger System based on Photovoltaic Module for Agricultural Electric Carriers

Eonuck Kang[1], Pandu Sandi Pratama[2], Jaeyoung Byun[1], Destiani Supeno[1], Sungwon Chung[1], Wonsik Choi[1]*

[1]Dept. of Bio-Industrial Machinery Engineering, Pusan National University, Miryang, Gyeongsangnam-do, Republic of Korea
[2]Live and Industry Convergence Research Inst., Pusan National University, Miryang, Gyeongsangnam-do, Republic of Korea

Received: October 17th, 2017; Revised: March 20th, 2018; Accepted: April 20th, 2018

Abstract

Purpose: In this study, a maintenance free super-capacitor battery charging system based on the photovoltaic module, to be used in agricultural electric carriers, was developed and its charging characteristics were studied in detail. **Methods:** At first, the electric carrier system configuration is introduced and the electric control components are presented. The super-capacitor batteries and photovoltaic module used in the experiment are specified. Next, the developed charging system consisting of a constant current / constant voltage Buck converter as the charging device and a super-capacitor cell as a balancing device are initiated. The proposed circuit design, a developed PCB layout of each device and a proportional control to check the current and voltage during the charging process are outlined. An experiment was carried out using a developed prototype to clarify the effectiveness of the proposed system. A power analyzer was used to measure the current and voltage during charging to evaluate the efficiency of the energy storage device. Finally, the conclusions of this research are presented. **Results:** The experimental results show that the proposed system successfully controls the charging current and balances the battery voltage. The maximum voltage of the super-capacitor battery obtained by using the proposed battery charger is 16.2 V, and the maximum charging current is 20 A. It was found that the charging time was less than an hour through the duty ratio of 95% or more. **Conclusions:** The developed battery charging system was successfully implemented on the agricultural electric carriers.

Keywords: Duty rate, Energy storage device, Maintenance free, Proportional control, Super-capacitor

Introduction

In recent years, manual transport vehicles have been used for short-distance transportation of harvested crops or cargoes. Many electric transport vehicles have gained popularity as material handling systems in industrial logistics and agricultural environment (Azwan et al., 2017; Chen et al., 2016; Moreda et al., 2016) for their efficiency in production and transportation of crops.

Generally, an electric vehicle is powered by a lead calcium or lead acid battery and a brushed motor installed at the axle of the differential gear of the wheel transmits power which is controlled by the control device of the motor driver performing the control functions of forward, reverse and speed. Batteries have high energy density but are hindered by slow dynamic response and low charge/discharge rates (Mendis et al., 2014). A super-capacitor can be an alternative solution to overcome this problem since it has high dynamic response and charge/discharge rates (Yassine and Fabris, 2017). Furthermore, its expected life is much longer than lead acid batteries since negligibly small chemical charge transfer reactions are involved (Kötz and Carlen, 2000). There have been several attempts to make a hybrid super-capacitor and battery (Kouchachvili et al., 2018), however, only a few researchers propose the super-capacitor as a battery replacement.

Owing to an improvement of up to 40% (King et al.,

***Corresponding author:** Wonsik Choi
Tel: +82-53-350-5425; Fax: +82-53-350-5429
E-mail: choi@pusan.ac.kr

2007) in the efficiency of photovoltaics (PVs), solar power has become a favorite alternative energy source to replace fuel and gas. There are many applications of the PV module in agricultural machinery such as crop dryers, solar water pumps, solar greenhouse heating, ventilation for livestock, solar aeration pumps, solar electricity (Hussain and Lee, 2015) and cultivators (Kim et al., 2014). The main problem in PV implementation lies in controlling the charging current and balancing the energy of each cell of the battery (Zhu et al., 2015). If the charging current is too high, the energy being supplied to the battery is no longer being consumed in the charge reaction, and must be dissipated as heat within the cell. This results in a very sharp increase in both the cell temperature and internal pressure if high current charging is continued. Due to manufacturing and assembly variances and operating conditions, the capacity of each battery cell is slightly different and without balancing, a cell of the smallest capacity could easily be overcharged or over-discharged while cells with higher capacities would only be partial charged. These conditions shorten the battery life and destroy the cells. However, not much research has been done to deal with this problem.

This study was, therefore, conducted to develop a super-capacitor battery charger system based on the PV module, especially for application in agricultural electric carriers. This research investigates the charging characteristics of the super-capacitor, which is the next generation core energy storage device, by comparing it with the lead acid battery, for which, a battery management system, charge control unit and a power supply switching unit were developed. In order to select two energy storage units, the power switching unit is applied by using a switching device. The charging characteristics were analyzed and compared with the generally used lead acid battery. The 120 W, 19.2 V single PV module was employed to charge the super-capacitor to 16.2 V using a constant current (CC) / constant voltage (CV) charging device so that the charging could be performed by utilizing a sufficient amount of sunshine from 10:00 am to 4:00 pm.

Materials and Methods

Electric carrier structure design

Mechanical configuration

The electric carrier used in this research (KW-B4D300, Keunwoo Tech Co. Ltd., Daegu, Rep. Korea) as shown in Figure 1 is modified four-wheel-drive electric cart. The frame of the vehicle was designed from high quality structural steel with a total body weight of 330 kg. The length and width of the vehicle were 1760 and 830 mm, respectively. The cargo size was 1220 mm (L)×800 mm (W)×220 mm (H) and total load capacity was 300 kg. The PV module was placed at the upper part of the vehicle to obtain maximum exposure to sunlight. The PV was installed at 1950 mm height. The super-capacitor was located at the lower part of the vehicle with the control

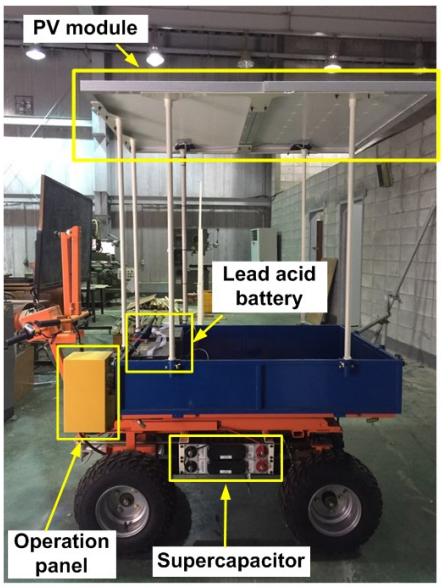

Figure 1. Configuration of electric carrier used in this study

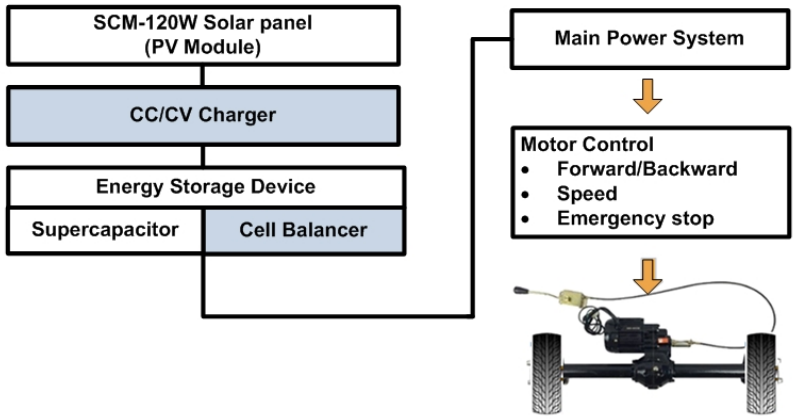

Figure 2. Schematic diagram of electric charging to use of power in the developed electric carrier

section of the operation panel in the front so that the controller could perform all the control operations.

Electrical configuration

The schematic diagram of the electrical configuration is shown in Figure 2. The proposed system was mainly powered by two 120 W PV module to deliver a maximum power of 240 W. The CC/CV charger was developed with a maximum capacity of 30 A (15 A × 2) to charge the super-capacitor with specific charging characteristics. Since the maximum production current generated from each PV module is 6.4 A, the maximum current from the PV module in this case was limited to 12.8 A leaving scope for development of a PV module with a power of 360 W (18 V×20 A) or more to reduce the charging time to half or less. The super-capacitor energy storage device consisted of two modules and each module consisted of 6 cell electric double-layer capacitor (LSUC 2.7V, LS-Mtron Ltd., Anyang, Gyeonggi-do, Rep. Korea) connected in series which has a total capacitance of 500 F and maximum voltage of 16.2 V for each module (LSUM 016R2C 0500F EA, LS-Mtron Ltd., Anyang, Gyeonggi-do, Rep. Korea). A cell balancer was used to prevent cell destruction of the super-capacitor and stabilize the balancing charge.

Photovoltaic module

Table 1 shows the specifications of the PV module (SCM 120WA, Solar Center Co. Ltd., Gimpo, Gyeonggi-do, Rep. Korea) used in this work. In accordance with the characteristics of the PV cell, 36 cells were connected to form a 4×9 matrix. Six poles with diameter ø3.5, thickness 1.5T (mm) and length 1000 mm were fixed to a support to configure the environment to bear the load.

The view of the PV cell and the support pillar are shown in Figure 1. The dimensions of the PV module were 660 mm (L) × 1143 mm (W) × 35 mm (H). The height of the support pillar is 1000 mm made of steel pipe with diameter 35 mm. The outer banding structure is added to increase the bonding force of the cell so that the whole frame could be set down.

Energy storage device

In this research work, the feasibility of replacing a lead acid battery (KB12100H, ENP Industrial Co. Ltd., Gumi, Rep. Korea) with the super-capacitor as an energy storage device is being examined. Table 2 presents a

Table 1. Specification of the PV module (SCM 120 WA)

Specification	Value
Maximum Power (P_{max})	120 W
Voltage at P_{max} (V_{mp})	19.2 V
Current at P_{max} (I_{mp})	6.4 A
Open-Circuit Voltage (V_{oc})	23.60 V
Short-Circuit Current (I_{sc})	6.93 A
Temperature Coefficient of V_{oc}	-(80±10) mV/°C
Temperature Coefficient of I_{sc}	(0.65±0.015)%/°C
Temperature Coefficient of Power	(0.5±0.005)%/°C
Operating temperature	-40°C to 85°C
Power tolerance	0/+5%

Table 2. Comparison of lead acid battery and super-capacitor

Characteristics	Lead Acid Battery	Super-Capacitor
Energy storage devices	E&P KB12100H (12 V 100 Ah)	LSUM 016R2C 0500F EA
Energy density (Wh/kg)	38 Wh/kg	3.3 Wh/kg
Max charging current	25 A	200 A
Charging time (100 Ah)	4 hour at 25 A	30 minute at 200 A
Equivalent Resistance	480 mΩ	1.7 mΩ
Operating temperature	-30~80℃	-45~65℃
Cycle life (0 < — > 100%)	260	1,000,000
Safety	not safe	safe
Environmental load	Pb	Active Carbon
Period of use	2~3 years	more than 60 years

comparison of some of their features. The charging current of the super-capacitor is about 8 times higher than that of the lead acid battery which means a lesser charging time of the former. Moreover, the super-capacitor is superior to the lead acid battery in terms of life cycle, safety, environmental load and period of use.

Super capacitor charging system design

Operation circuit for cell balancing of the super-capacitor

A balanced stabilization charging control of all the six cells is required to prevent cell destruction of the super-capacitor and maintain a stable balancing charge. Stable charging means that the maximum buffering voltage of each cell is 2.7 V. If the voltage exceeds the permissible value, the cell is destroyed and it is difficult to secure stability of operation. The battery management system (BMS) function is known as a key technology for lithium-ion battery or super-capacitor energy storage device because the charging voltage is different for each cell. However, in order to use each cell, the six cells must be connected in series to produce a separate cell balance. In this study, a separate cell balancing circuit was designed and applied.

The active cell balancing circuit used in this research is shown in Figure 3. This circuit consists of 6 identical circuits connected in parallel to each super-capacitor. For the sake of simplicity, only the circuit connected to the super-capacitor having the highest voltage and that connected to the last super-capacitor is shown in this figure. 'Un' in the schematic are the voltage detector ICs (BD4823G, ROHM Co. Ltd., Kyoto, Japan) used as balancing charge controls. If the voltage is less than the permitted limit, a chip enabled signal is applied to the gate of 'Qn' to allocate the drain current (I_d) to each cell of the right super-capacitor. The drain current is shown in red arrow in Figure 3. When the permitted voltage is exceeded, since the FET is not operated, the battery is not charged any more. The current then fill the capacitor on the right side as shown in green arrow in Figure 3. By this principle, cell balancing of all the cells is maintained. Figure 4 shows a stable cell balance circuit and the PCB layout.

Development of CC / CV charger for the super capacitor

The equivalent circuit of CC/CV charger is shown in Figure 5. The switch used on the right side is a step-down type DC / DC buck converter that converts an input voltage of 8 V to 40 V to provide a stable output voltage in the range of 1.25 V to 36 V using the switching regulator chip (XL4016, XLSEMI, Shanghai, China). Pulse width modulation of maximum duty cycle of 100% is applicable. This device works at a fixed switching frequency of 180 kHz. The constant current output capability is 8 A. To provide higher currents, the output sink can be further extended to reduce the heat generated by the switching device. The output voltage V_{OUT} at the last node is applied to the super-capacitor.

The total current applied to each super-capacitor by the DC connection defined in the KCL (Kirchhoff Current Law) of the super-capacitor is I. The serial charge current of the super-capacitor connected to the V_{OUT} node for charging can be briefly defined by the following equation.

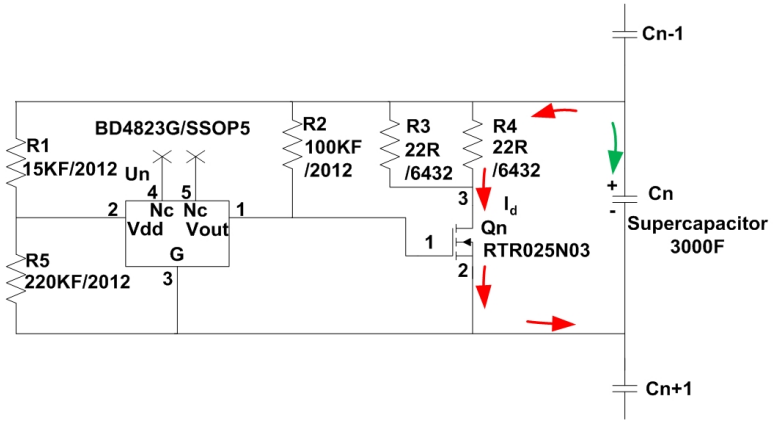

Figure 3. Single super-capacitor cell balancing circuit

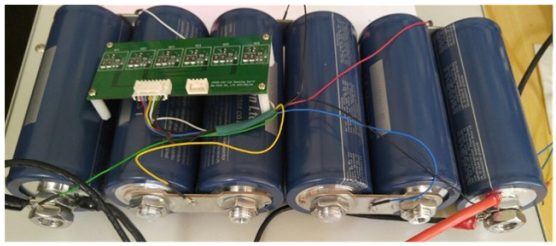

Figure 4. Developed active balancing PCB connected to super-capacitor

$$\frac{dV_{OUT}}{dt}=\frac{dV_1}{dt}+\frac{dV_2}{dt}+\cdots+\frac{dV_n}{dt}$$
$$=\frac{I}{C_1}+\frac{I}{C_2}+\cdots+\frac{I}{C_n} \quad (1)$$
$$=\left(\frac{1}{C_1}+\frac{1}{C_2}+\cdots+\frac{1}{C_n}\right)I=\frac{I}{C_{eq}}$$

where $V_1, V_2, \cdots, V_n$ are the voltages of each capacitor, $C_1, C_2, \cdots, C_n$ are the capacitances of each capacitor, and C_{eq} is the equivalent capacitance.

Figure 6 shows the circuit extracts netlist based on OrCAD16.6 (Cadence Design Systems Inc., San Jose, CA, USA). The input power for the experiment is 24 V DC. The output voltage of the buck converter was trimmed by adjusting the variable resistor VR1 value at the rated permissible voltage of the super-capacitor of 16.2 V (2.7 V × 6 Cells). In addition, the current limit is set to 8 A by using the variable resistor VR2, and input power is applied to check the output value.

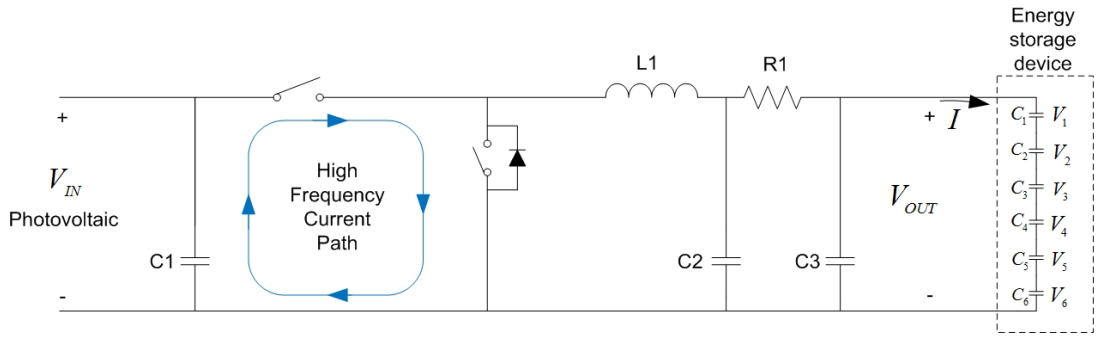

Figure 5. Equivalent circuit of CC/CV charger

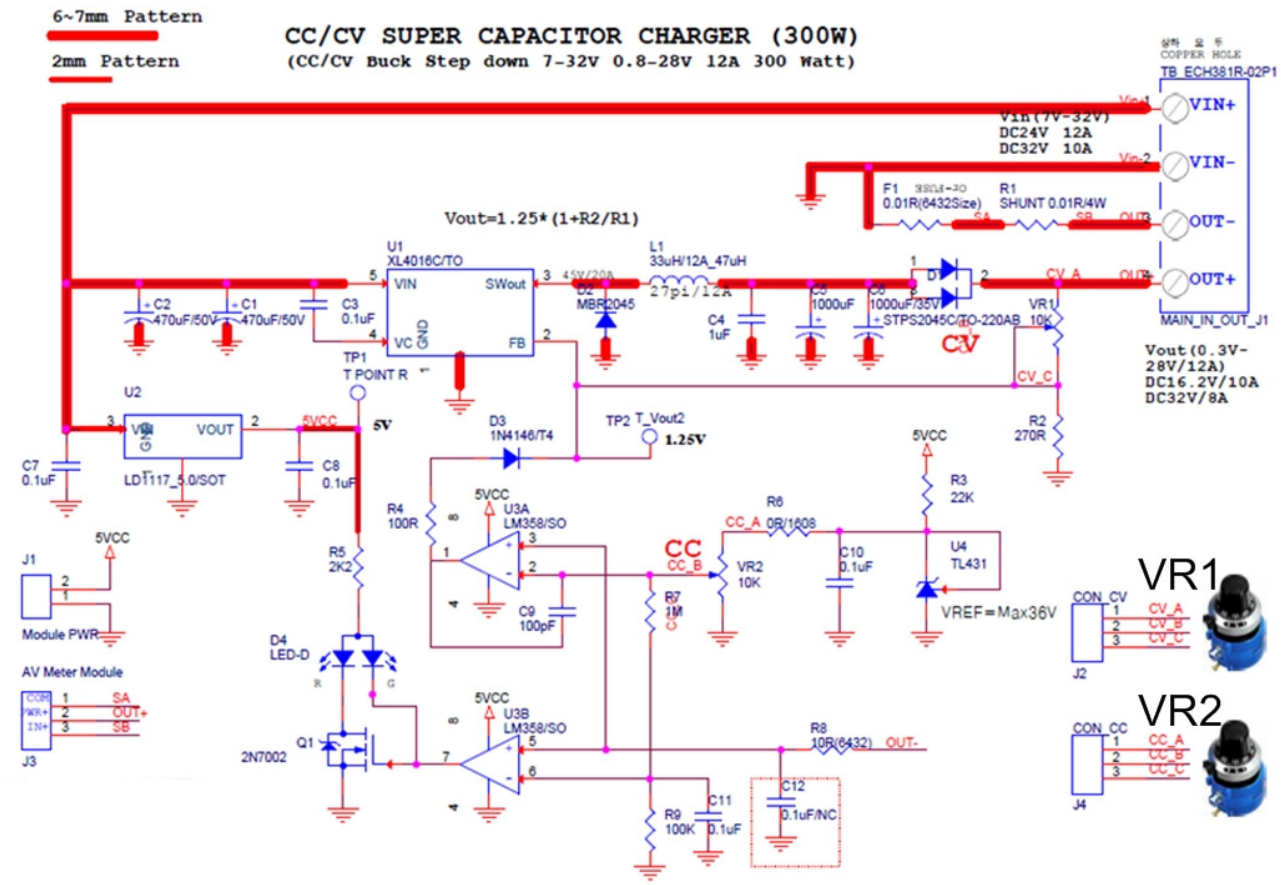

Figure 6. Circuit design for the CC/CV supercapacitor charger

CC / CV charger standby power circuit technology

The super-capacitor was charged gradually by using the CC / CV charger linearly with the charge profile as in (Barsukov and Qian, 2013), keeping within the range of the maximum allowable voltage. It is difficult to guarantee the lifetime of the capacitor unless the range is maintained. Therefore, it is necessary to apply the V-charge according to the time domain (CV) and to cut-off charging by reducing the current when the maximum voltage is reached (CC).

When the external charging power source is not applied or the battery is in a standby state in which the operation is idle, there occurs a situation in which the battery or the energy stored in the energy storage device leaks backward. The XL4016 used in this development can cut off the limited current control through the feedback pin of the 2nd pin, and the VR1. Since the OP-amp, which is networked in VR2, is controlled, external power leakage can be prevented. When it is used in industrial applications, discharge leakage current, including self-consumption power, is not allowed to be more than 40 mA.

Experimental environment

In order to verify the stable charging operation, the experiment of the electric vehicle was carried out through the PV after the development. The experimental setup consists of two PV modules, two batteries and two modules of supercapacitors in series attached on the electric carrier as shown in Figure 1. The experiment was done with all components installed on the electric carrier. The selection switch, CC/CV charger, cell balancer are connected as shown in Figure 7. The charging current and voltage was measured during experiment using a power analyzer (WT500, Yokogawa Electric Corp., Tokyo, Japan). The data then sent to the computer through the Ethernet. WTViewerE software (Yokogawa Electric Corp., Tokyo, Japan) enables computer to visualize the data and to monitor the data acquisition. The global solar irradiance was measured during experiment using a Solar Power Meter (TES-132, TES Electrical Electronic Corp., Taipei, Taiwan). The accuracy is typically ±10 W/m^2 and additional temperature induced error ±38 W/m^2/°C from 25°C. The sampling rate of this measurement device is 1 time/sec. Two lead acid batteries with maximum voltage of 12 V and capacity of 100 Ah were used as comparison. To clarify the maximum performance of super capacitor, the programmable power supply with maximum rate 100V/60A (KSC-6KW, Korea Switching Co. Ltd., Seoul, Rep. Korea) was applied to conduct the experiment. A selection switch that could withstand DC 24 V, 50 A in the maximum test environment was used between the energy storage and main power system. This configuration enabled selection between the super-capacitor and lead acid battery during the experiment. In addition, it had a switchable toggle switch that had a tolerance of 600 V. In this research five test conditions was done:

1. Cell balancing test
2. Super-capacitor charged by power supply
3. Lead acid battery charged by power supply

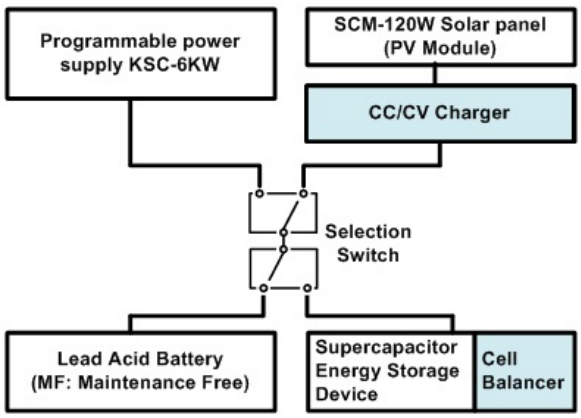

Figure 7. Experimental schematics for charging characteristics comparison between super-capacitor and lead-acid battery

Table 3. Fully charged cell voltage using active balancing method

Ref no.	Cell Number	Final voltage (V)
1	Cell1	2.701 V
2	Cell2	2.699 V
3	Cell3	2.700 V
4	Cell4	2.701 V
5	Cell5	2.698 V
6	Cell6	2.700 V

4. Super-capacitor charged by photovoltaic
5. Lead acid battery charged by photovoltaic

Results and Discussion

In this experiment, the main input voltage used was DC24, the maximum constant current was set at 10A and the charge test was performed at zero voltage after full discharge. The results of this test are shown in Table 3 which include the final voltage of each cell at the end of the experiment. The result of the experiment showed that the maximum value was stable for each cell. The range of error in the voltage measurement in Table 3 is ± 0.03 V.

Figure 8 shows the charging of the super-capacitor using the power supply. A full charge is attempted by applying power to the power supply at an initial super-capacitor discharge state of 0 V. In the beginning, the charging uses a constant current of about 10 A. When it is charged up to 16 V, the charging mode is constant voltage.

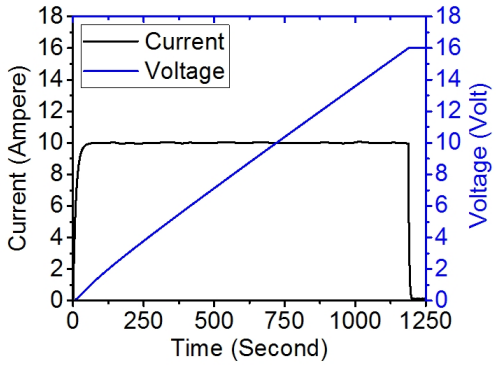

Figure 8. Charging data of super-capacitor charged by power supply

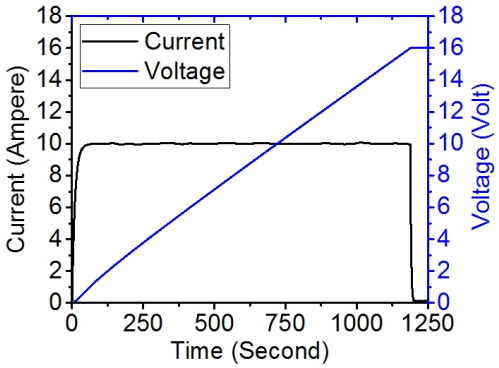

Figure 9. Charging data of battery charged by power supply

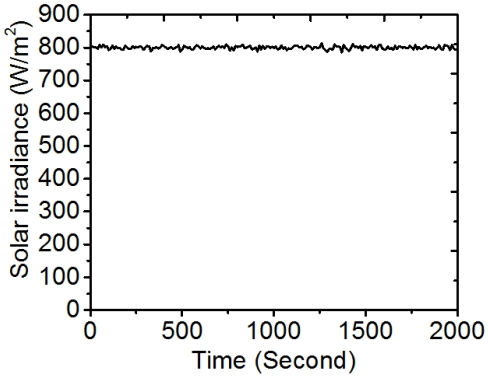

Figure 10. Solar irradiance during experiment

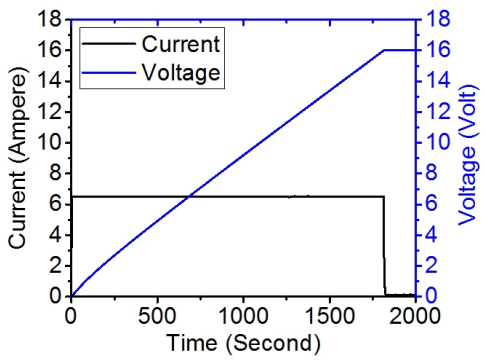

Figure 11. Charging data of super-capacitor charged by photovoltaic

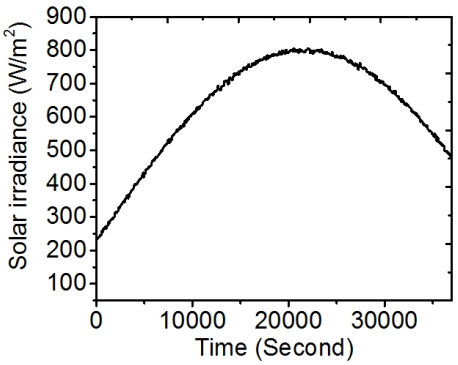

Figure 12. Solar irradiance during experiment

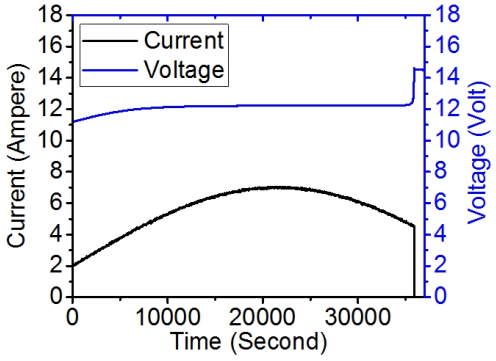

Figure 13. Charging data of battery charged by photovoltaic

At this time the charging current decreases and drops to zero.

Figure 9 shows the charging of the battery by using the power supply. A full charge is attempted by applying power to the power supply at an initial battery discharge state of 11.2 V. In the beginning, the charging uses a constant current of about 10 A. When it is charged up to 14.5 V the charging mode is constant voltage. At this time the charging current decreases and drops to zero.

Figure 10 shows the solar irradiance obtained during the experiment. The ambient temperature of the air was 20°C. The experiment was done at 12 PM during midday to obtain maximum solar irradiance. In Figure 11 the charging graph by the PV module shows the power generated and sent to the charger. The voltage and current are measured every minute, and the voltage gradually increases at a certain rate. The buck charger checks the process once the maximum 16.2 V is reached. The charging current does not exceed 6.5 A because that is the current produced by the PV module. A constant current trimming of less than 40 mA is required since the switching frequency of the buck converter is high and a small duty cycle could not be obtained due to Minimum On-Time Period of the switching device. Moreover, current trimming was done to minimize switching losses and to extend the life of the charging system.

Figure 12 shows the solar irradiance obtained during the battery charging experiment. The ambient temperature of the air was 20°C. The experiment was conducted from 8 am to 4 pm. In Figure 13 the charging graph of the PV module is shown. Since the capacity of the battery is larger than that of the super-capacitor, more time is required to fully charge the battery.

Conclusions

In this study, a maintenance free super-capacitor battery charging system based on the PV module used in agricultural electric carriers was developed. Super-capacitor cell balancing based on active balancing method and super-capacitor CC/CV charger based on buck converter technology was proposed. The main results were obtained as follows:

1. The experimental result shows that the system was successfully implemented on the agricultural electric carriers.
2. The developed capacitor voltage balancing successfully distributed the voltage and the average voltage of each cell was 2.700 V with an error of ± 0.03 V.
3. The proposed Super-capacitor CC / CV charger successfully charged the battery and the experimental result shows that the fully charged super-capacitor battery voltage was 16.201 V.
4. The charging currents were varied according to the battery voltage and the maximum charging current was 10 A. These values satisfied the safety current and voltage norms of battery operation.

Conflict of Interest

The authors have no conflicting financial or other interests.

Acknowledgement

This research was supported by the Ministry of Agriculture, Food and Rural Affairs Research Center of Republic of Korea Government.

References

Azwan, M. B., A. L. Norasikin, K. Sopian, S. Abd Rahim, K. Norman, K. Ramdhan and D. Solah. 2017. Assessment of electric vehicle and photovoltaic integration for oil palm mechanisation practise. Journal of Cleaner Production 140(3): 1365-1375. https://doi.org/10.1016/j.jclepro.2016.10.016

Barsukov, Y. and J. Qian. 2013. *Battery Power Management for Portable Devices*, Norwood, MA, USA: Artech House Inc.

Chen, Y., B. Xie and E. Mao. 2016. Electric tractor motor drive control based on FPGA. IFAC-PapersOnLine 49(16): 271-276. https://doi.org/10.1016/j.ifacol.2016.10.050

Hussain, M. I. and G. H. Lee. 2015. Utilization of solar energy in agricultural machinery engineering: A review. Journal of Biosystems Engineering 40(3): 186-192. http://doi.org/10.5307/JBE.2015.40.3.186

Kim, S. C., Y. K. Hong and G. H. Kim. 2014. Environmentally

friendly hybrid power system for cultivators. Journal of Biosystems Engineering 39(4): 274-282. https://doi.org/10.5307/JBE.2014.39.4.274

King, R. R., D. C. Law, K. M. Edmondson, C. M. Fetzer, G. S. Kinsey, H. Yoon, R. A. Sherif and N. H. Karam. 2007. 40% efficient metamorphic GaInP/GaInAs/Ge multijunction solar cells. Applied Physics Letters 90: 183516. https://doi.org/10.1063/1.2734507

Kötz, R. and M. Carlen. 2000. Principles and applications of electrochemical capacitors. Electrochimica Acta 45(15-16): 2483–2498. https://doi.org/10.1016/S0013-4686(00)00354-6

Kouchachvili, L., W. Yaïci and E. Entchev. 2018. Hybrid battery/supercapacitor energy storage system for the electric vehicles. Journal of Power Sources 374: 237-248. https://doi.org/10.1016/j.jpowsour.2017.11.040

Mendis, N., K. M. Muttaqi and S. Perera. 2014. Management of low- and high-frequency power components in demand-generation fluctuations of a DFIG-based wind-dominated RAPS system using hybrid energy storage. IEEE Transactions on Industry Applications 50(3): 2258-2268. https://doi.org/10.1109/TIA.2013.2289973

Moreda, G. P., M. A. Muñoz-García and P. Barreiro. 2016. High voltage electrification of tractor and agricultural machinery – A review. Energy Conversion and Management 115: 117-131. https://doi.org/10.1016/j.enconman.2016.02.018

Yassine, M. and D. Fabris. 2017. Performance of commercially available supercapacitors. Energies 10(9): 1340. https://doi.org/10.3390/en10091340

Zhu, H., D. Zhang, H. S. Athab, B. Wu and Y. Gu. 2015. PV isolated three-port converter and energy-balancing control method for PV-battery power supply applications. IEEE Transactions on Industrial Electronics 62(6): 3595-3606. https://doi.org/10.1109/TIE.2014.2378752